CHEMICAL ENGINEERING TRANSACTIONS
VOL. 39, 2014
A publication of AIDIC
The Italian Association of Chemical Engineering
www.aidic.it/cet
Guest Editors: Petar Sabev Varbanov, Jiří Jaromír Klemeš, Peng Yen Liew, Jun Yow Yong

ISBN 978-88-95608-30-3; **ISSN** 2283-9216
DOI: 10.3303/CET1439227

Infrared Thermography and CFD Analysis of Hydrocarbon Jet Fires

Luis G. Zárate*[a], Hugo E. Lara[a], Mario E. Cordero[a], Bulent Kozanoglu[b]

[a]Universidad Popular Autónoma del Estado de Puebla, 21 Sur 1103, Barrio de Santiago, 72410, Puebla, Puebla, México
[b]Universidad de las Américas-Puebla, Ex hacienda Santa Catarina Martir, 72820, Puebla, México
luis.zarate@upaep.mx

Fire modelling requires integrating the behaviour of hydrodynamics, heat and mass transfer as well as the combustion reaction. In the present paper, Jet Fires have been studied through CFD analysis, using the Reynolds-Averaged Navier-Stokes (RANS) equations, coupled with a $\kappa-\varepsilon$ turbulence model. The energy transport equation includes radiation terms. The temperature values obtained have shown an acceptable agreement with the experimental results obtained by IR thermography. Total heat flux values have also been analysed, indicating that there are some limitations in the model.

1. Introduction

One of the most distinctive characteristics of a jet fire is a turbulent diffusion flame which is originated from the combustion of a fuel that continuously escapes by a velocity, ranging from subsonic, in some rare cases, to supersonic states and creating an amount of movement in a certain direction. Jet fires can result from gas, liquid or two-phase mixture emissions. The behaviour of jet fires depends on fuel composition, release conditions, mass flow rate, geometry of the orifice and weather conditions.

The importance of jet fire research resides in its frequent presence in industrial applications as well as in major accidents, where high heat fluxes can seriously affect facilities and leading to, in most of the cases, a domino effect (Gomez et al., 2008). Jet fires are often used in hydrocarbon process plants in order to eliminate non-desirable gases during petroleum extraction cycles (production torches). In hydrocarbon refining and petrochemical plants they are used to eliminate by-products through security valves (process torches). They can be also employed to regulate a controlled unit operation such as ovens, gas turbines or industrial burners. On the other hand, referring to major accidents, historical statistics show that 50 % of accidental jet fires caused a domino effect; 90 % of them leading to an explosion (Casal et al., 2012).

This type of accidents had been widely studied for decades. Ricou and Spalding (1961) made direct measurements of entrainment by axisymmetric turbulent jets. Brzustowski (1973) proposed equations to predict flame shapes of a gaseous turbulent diffusion flames. Chamberlain (1987) presented models to study flare flame shapes and radiation fields. Cook et al. (1987) made experimental and theoretical studies of flare dimensions and heat radiation. Chamberlain's model was later extended by Johnson et al. (1994) to describe a horizontal jet flame of natural gas.

Apart from experimental studies, like Gomez (2009) who analysed radiative heat transfer, or Palacios (2011) who studied flame geometries, a different approach to jet fire analysis also can be carried out by the employment of computer simulation, implementing various numeric algorithms capable of simultaneously solving hundreds of equations (Modest, 2008). Some simulations were performed using unsteady RANS with different turbulence models coupled with chemistry and radiation models, demonstrating that CFD (Computational Fluid Dynamics) tools have become a great potential aid (Broukal et al., 2012). The advantage of computational modelling resides in the prediction of the fire behaviour (action radio, thermal effects) with substantial money and time savings, also, in avoiding risky situations when field experiments carried out. But it is also important to mention that fire modelling is very complex (Tavelli et al., 2014), and these models present limited applicability due to extremely high computational

Please cite this article as: Zárate L.G., Lara H.E., Cordero M.E., Kozanoglu B., 2014, Infrared thermography and CFD analysis of hydrocarbon jet fires, Chemical Engineering Transactions, 39, 1357-1362 DOI:10.3303/CET1439227

burdens added through the presence of turbulent flows and non-stoichiometric mixtures (Tugnoli et al., 2013). The high degree of variability in length and time scales also contributes to the complicated nature of the problem (Magnussen et al., 2013).

2. Methodology

2.1 Infrared thermography

The experimental facilities are located in “Can Padró” Center for Security Education, in the province of Barcelona, Catalonia, Spain. The fuel selected as test material was propane which was burned using different nozzle diameters in order to obtain different sizes of jet fires.

All the experiments were recorded with an AGEMA 570 thermal camera which uses a Focal Plane Array of 320x240 pixels. This type of thermal camera captures the infrared radiation transmitted from a hot object and then transforms the received information in high resolution images where a point-temperature value corresponding to each pixel of the recorded image. The data acquisition system also includes a meteorological station in order to register the weather conditions. Further details about the experimental facilities can be consulted elsewhere (Palacios, 2011).

2.2 CFD simulation

Jet fire modelling has to include the important spatial and time relating variations that take place during the phenomenon in a turbulent-reacting flow. The approach of this paper is to simulate the different phenomena in the combustion zone, just above the area where the jet nozzle is located. This region appears when the local mixture of vaporized fuel and air react to generate combustion products and energy. A complete focus on the problem must contain the momentum, energy and mass transport equations as well as the combustion phenomenon. In this work, the first two phenomena were taken into the consideration, leaving the mass transport and combustion phenomena for further research. The study contemplates the Reynolds-Averaged Navier Stokes (RANS) transport equations and a κ–ε turbulence model. The energy transport equations include the radiation term.

2.3 Hydrodynamics model

The Reynolds-Averaged Navier Stokes (RANS) transport equations are utilized in order to predict the turbulent behavior of jet fires, the general equations are as follows:

$$\rho\frac{\partial U}{\partial t}+\rho U\cdot\nabla U+\nabla\cdot(\rho\bar{u}'\bar{u}')=-\nabla P+\nabla\cdot\mu(\nabla U+(\nabla U)^T)+F \tag{1}$$

$$\nabla\cdot U=0 \tag{2}$$

where U is the average field velocity (m/s); F is the body force vector (N/ m^3). The interactions between velocity fluctuations (also called Reynolds Shear Tensor) are described by the term between brackets($\rho\bar{u}'\,\bar{u}'$).

The RANS equations are solved simultaneously with the turbulent κ–ε model Eq(3) and Eq(4), it becomes necessary to include the kinetic turbulent energy κ and the dissipation factor ε. This model considers the turbulent viscosity as follows: $\mu_T=\rho C_\mu(\kappa^2/\varepsilon)$ where C_μ is a constant value.

$$\rho\frac{\partial k}{\partial t}-\nabla\cdot\left[\left(\mu+\frac{\mu_T}{\sigma_k}\right)\nabla k\right]+\rho U\cdot\nabla k = \frac{1}{2}\mu_T(\nabla U+(\nabla U)^T)^2-\rho\varepsilon \tag{3}$$

$$\rho\frac{\partial \varepsilon}{\partial t}-\nabla\cdot\left[\left(\mu+\frac{\mu_T}{\sigma_\varepsilon}\right)\nabla \varepsilon\right]+\rho U\cdot\nabla \varepsilon = \frac{1}{2}C_{\varepsilon 1}\frac{\varepsilon}{k}\mu_T(\nabla U+(\nabla U)^T)^2-\rho C_{\varepsilon 2}\frac{\varepsilon^2}{k} \tag{4}$$

Valid constant values for Eq(3) and Eq(4) are encountered in the technical literature and were obtained by experimental data (Aglave R., 2007):

$$C_\mu=0.09,\qquad C_{\varepsilon 1}=1.44,\qquad C_{\varepsilon 2}=1.92,\qquad \sigma_k=1.0,\qquad \sigma_\varepsilon=1.3 \tag{5}$$

The validity of Eq(1) to Eq(4) resides in the need of a fully developed turbulent flow with equilibrium boundaries, which means that the turbulence is equivalent to dissipation rates (this does not apply for all jet fires).

2.4 Energy transport model

For this model, the general energy transport equation Eq(6) is used, considering all thermal energy effects (inlets, outlets and generation):

$$\nabla \cdot k\nabla T + q + \Phi = \rho C_v \frac{DT}{Dt} + v \cdot \mu \nabla^2 v \quad (6)$$

where Φ denotes the viscous work rate per unit volume and q is the thermal energy generation rate per unit volume (W/m^3).

2.5 Mass transport model

$$\frac{\partial c_i}{\partial t} + \nabla \cdot \left(-D_i \nabla c_i\right) = R_i - u\nabla \cdot c_i \quad (7)$$

In Eq(7), D_i represents the diffusion coefficient of component i (m^2/s), c_i is the concentration of component i, while R_i is the production rate of the component i (mol/m^{3}s).

Although CFD techniques can predict the hydrodynamic behaviour of a jet fire (as well as its shape and size) its implementation becomes very complicated. Because of this, in the first stage of this research, the use of the solid body model has been chosen. Using this model results in a small deviation from experimental data (Casal, 1999). In addition, looking for a reduction in number of elements in the grid, and mathematical operations to be done, the simulation is considered axisymmetric, simulating only half of the jet fire domain proposed.

Table 1: Selected boundary conditions for the hydrodynamics model

Boundary	Boundary condition	Condition description
1,2	Wall, inexistent fluid-flame viscous interactions	Characteristic eddy length and turbulence intensity values are added
5	Specified inlet velocity	$u = -nU_0$
3,4	Open boundary (convective flow only)	$(\eta + \eta_T)$ $n \cdot \nabla k = 0$ $(\nabla u + (\nabla u)^T)n = 0$ $n \cdot \nabla \varepsilon = 0$

Table 2: Selected boundary conditions for the heat transfer model

Boundary	Boundary condition	Condition description
1,4	Thermal insulation	$-n \cdot (-k\nabla T) = 0$
2	Specified heat flux	$-n \cdot (-k\nabla T) = q_0$
5	Specified temperature	$T = T_0$
3	Convective flow	$q_{cond} \cdot n =$ $-k\nabla T \cdot n = 0$ $q \cdot n = \rho Cp\left(uT \cdot n\right)$

The sequence used for the Jet Fire simulation can be appreciated in Figure 1, where (a) displays Domain characterization and (b) presents establishment of boundary conditions. The boundary conditions assigned to the hydrodynamics as well as to the heat transfer models are indicated in Table 1 and Table 2, respectively. Figure 1(c) shows the grid generation throughout the selected domain. The following step is solving the transport equations mentioned earlier in this paper and obtaining results, as shown in (d), over temperature and velocity profiles. These values are then plotted in Figure 2 where non-dimensional flame length values are considered. According to this consideration, the maximum length value corresponds to 1, while *x* values of 0.1, 0.2, 0.3 and 0.4 are representing the 10 %, 20 %, 30 % and 40 % of the total flame length. It also can be observed from Figure 2 that low temperature values were registered in the lower part of the simulated region, and then rapidly increasing temperature values are observed in the region considered as the low part of the “solid” flame, reaching values around 1,500 °C. The temperature values decrease also in the zones far from the flame region.

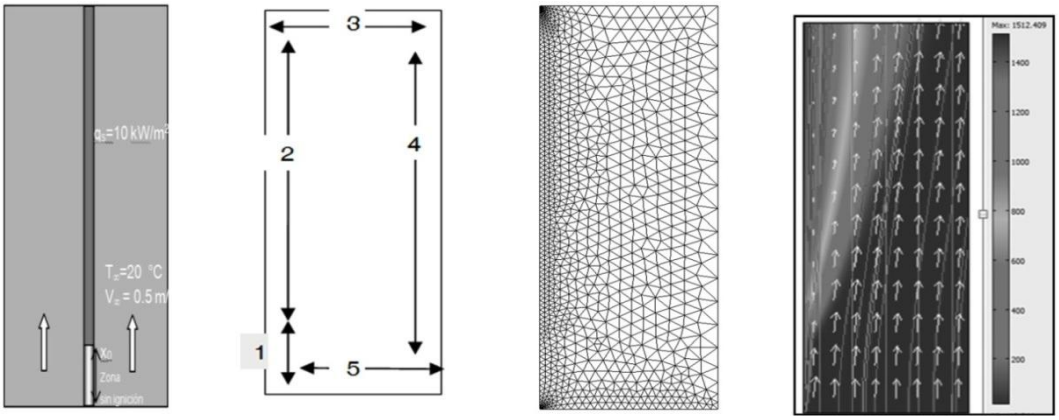

(a) 2D Approach (b) Geometry domain and boundary conditions (c) Triangular mesh (d) Temperature and momentum profiles.

Figure 1: Jet Fire simulation sequence

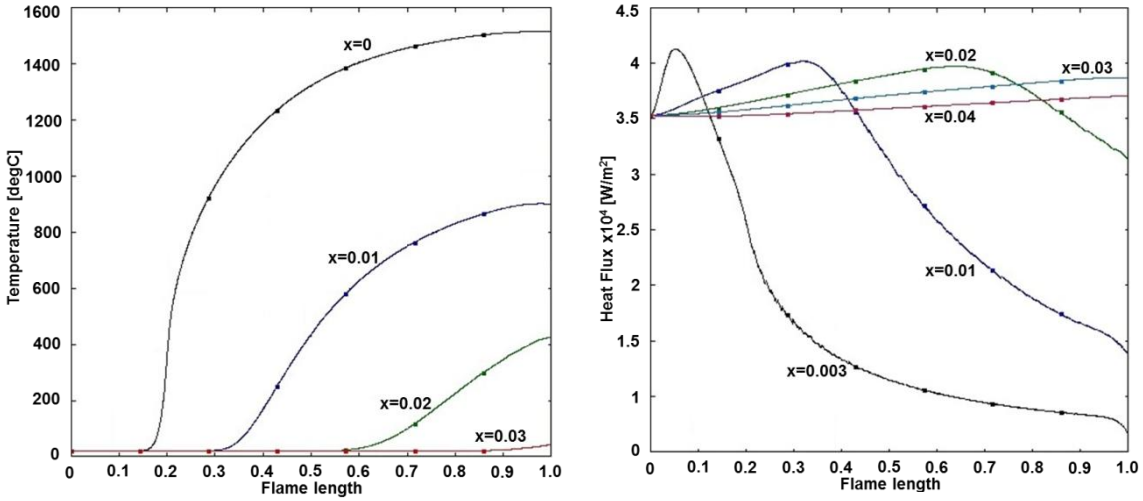

(a) Temperature profiles *(b) Total heat flux profiles*

Figure 2: Profiles obtained from CFD simulation

Figure 2 shows the variation of the total heat flux as a function of the flame length. The total heat flux includes the thermal convection and radiation mechanisms expressed in W/m^2. The maximum heat flow rates (with values approaching 40 kW/m^2) reached in the flame zone can be seen decreasing their values as the distance from the flame increases. In curves x=0.003 and x=0.01 the values decrease drastically, since the profiles selected are parallel lines that are located very near the flame surface. For this reason, both curves have made contact with the boundary of the model; the turbulent model is not able to represent the velocities in this region correctly.

The experimental values taken from infrared thermal images are shown in Table 3. It is important to denote that the results from the CFD simulation have the same order of magnitude as the values presented in this table. Nonetheless, it is important to mention that the experimental conditions should coincide with the conditions of the simulation to be really able to compare these values, which is out of the scope of the present work.

Table 3: Experimental temperature values of infrared images

Height %	Temperature (K)
Jet source-20	1,200-1,400
20-40	1,400-1,600
40-60	1,600-1,800
60-80	1,450-1,650
80-100	1,500-1,600

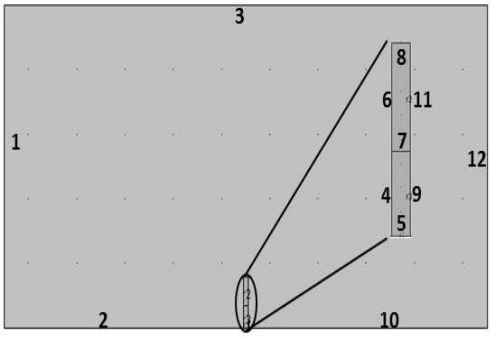

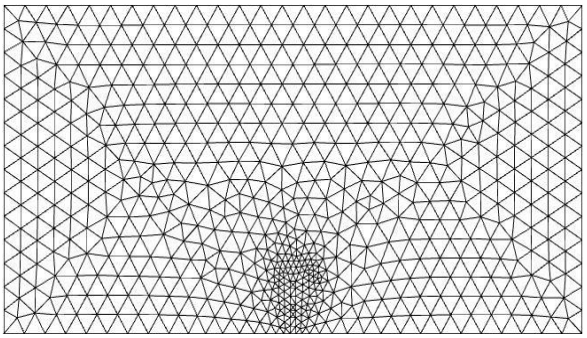

Figure 3: Boundary conditions, extended zone. *Figure 4: Final mesh consisting of 1,238 elements.*

It is also possible to modify the geometry and boundary conditions of the simulation shown in Figure 1. The experiments that were considered presented height fluctuations between 2 and 8 meters, while the mass flow ranged between 0.05-0.4 kg/s. The second proposed geometry uses the same heat and momentum transport equations and turbulent models. Figure 3 shows the new geometry with its inherent new considerations. Open boundaries 1, 3 and 12 denote that fluid can either enter or exit through these boundaries. The boundaries 2 and 10 describe an air inlet at ambient temperature, while boundaries 4, 6, 9 and 11 are no-slip wall condition boundaries for the momentum transport model. Boundary 5 denotes a fuel inlet (for this simulation, propane has been selected as fuel). Boundary 8, represents the fuel (propane) outlet. The final mesh configuration, consisting of 1,238 independent mesh elements is shown in Figure 4.

Hydrodynamics results obtained from this simulation are shown in Figure 5. The maximum momentum rate is observed at the nozzle, with a value of 50 m/s; this value decreases as the flame height increases, maintaining the maximum velocity at the jet centre.

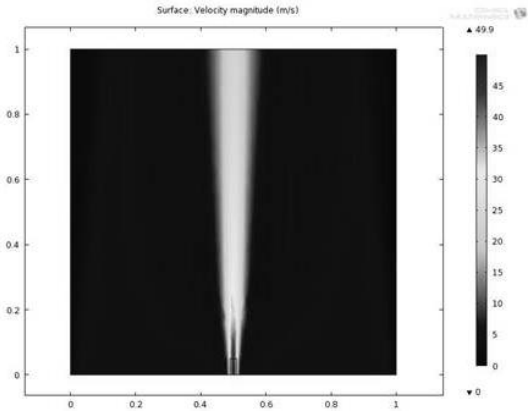

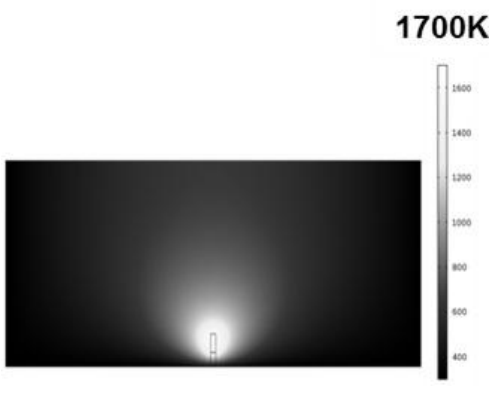

Figure 5: Jet Hydrodynamics. *Figure 6: Jet fire temperature profiles.*

Figure 6 shows the inherent results from the heat transfer model. The maximum temperature value is 1,700 K. As expected, the maximum values were obtained around the central axis of the jet, decreasing its value as the position from the jet axis increases. This temperature values show similar orders of

magnitude and behaviours with the experimental temperature values obtained through the thermal images, presented in Table 3.

3. Conclusions

Jet fire simulations including heat, momentum and mass transport were realized. The solid flame model was used in order to reduce computing complexity and to represent the zone out of the flame. Results show similar behaviours and tendencies with the experimental values obtained by thermo graphic methods, the temperatures are being between 1,600 and 1,700K. Nevertheless, this model was not able to reproduce the experimental point-temperature values that are above the maximum temperature interval that was mentioned earlier.

The combustion model of propane jet fire took into account a stoichiometric combustion and parallel air inlets. The maximum velocity value (50 m/s) was located at the nozzle, decreasing with the distance from the nozzle, maintaining a local maximum velocity at the centre of the jet. However, it is necessary to improve the heat transport results since they do not reproduce the experimental flame behaviour.

These models are able to produce values in the entire simulated region, in contrast with the limited amount of data obtained by experimentation, showing that CFD simulation techniques represent a good option to study this type of phenomena. However, some convergence-reaching strategies must be considered, in view of not committing excessive simplifications, resulting in a non-representative simulation. In addition, all the assumptions must be coherent; otherwise, a valid solution for the model will never be reached.

References

Aglave R., 2007, CFD simulation of combustion using automatically reduced reaction mechanisms: A case for diesel engine, PhD Thesis, University of Heidelberg, Germany

Broukal J., Vondàl J., Hàjek J., 2012, Experimental and numerical investigation of wall heat fluxes in a gas fired furnace: practicable models for swirling non-premixed combustion, Chemical Engineering Transactions, 29, 1399-1404

Brzustowski T.A., 1973, Anew criterion for the length of a gaseous turbulent diffusion flame. CombustionScience and Technology, 6, 313–319

Casal J., Gomez-Mares M., Munoz M., Palacios A., 2012, Jet fires: a “minor” fire Hazard?, Chemical Engineering Transactions, 26, 13-20

Casal J., Montiel H., Planas E., Vílchez J.A., 1999, Risk analysis in industrial facilities, Ediciones UPC, Barcelona, Spain (in Spanish)

Chamberlain G.A., 1987, Developments in design methods for predicting thermal radiation from flares. Chemical Engineering Research and Design, 65, 299–309

Cook D.T., Fairweather M., Hammonds J., 1987, Size and radiative characteristics of natural gas flares, Chemical Engineering Research and Design, 65, 310-318

Gómez M.M., Zárate L., Casal J., 2008, Jet fires and the domino effect. Fire Safety Journal, 43, 8, 583-588

Gómez M.M., 2009, Jet fires experimental studies and numerical simulations, PhD Thesis, UPC, Barcelona, Spain (in Spanish)

Johnson A.D., Brightwell H.M., Carsley A.J., 1994, A model for predicting the thermal radiation hazards from large-scale horizontally released natural gas jet fires. Hazards, 13, 123

Magnussen B.F., Rian K.E., Grismsmo B., Lilleheie N.I., Kleiveland R.N., Vembe B.E., 2013, Computational analysis of large-scale fires in complex geometries – a means to safeguard people and structural integrity in the oil and gas industry, Chemical Engineering Transactions, 31, 793-798

Modest M.F., 2008, Radiative heat transfer in fire modeling. Transport Phenomena in Fires. WITPRESS, Boston, USA

Palacios A., 2011, Study of jet fires geometry and radiative features. Ph. D. Thesis, UPC, Barcelona, Spain

Ricou F.P., Spalding D.B., 1961, Measurements of entrainment by axisymmetrical turbulent jets. Journal of Fluid Mechanics, 8, 21–32

Tavelli S., Rota R., Derudi M., 2014, A critical comparison between cfd and zone models for the consequence analysis of fires in congested environments, Chemical Engineering Transactions, 36, 247-252

Tugnoli A., Salzano E., Di Benedetto A., Russo P., Cozzani V., 2013, Analysis of the flash-fire scenario in the viareggio accident, Chemical Engineering Transactions, 32, 403-408.